RIVER RESEARCH AND APPLICATIONS

River. Res. Applic. **23**: 407–427 (2007)

Published online 31 January 2007 in Wiley InterScience
(www.interscience.wiley.com) DOI: 10.1002/rra.983

FLOOD FREQUENCY AND ROUTING PROCESSES AT A CONFLUENCE OF THE MIDDLE YELLOW RIVER IN CHINA

HONGMING HE,[a] JIE ZHOU,[a] QIAN YU,[b] YONG Q. TIAN[c]* and ROBERT F. CHEN[c]

[a] *State Key Laboratory of Loess and Quaternary Geology, Institute of Earth Environment, Chinese Academy of Sciences, P. O. Box 17, Xian, 710075, China*

[b] *Department of Geosciences, University of Massachusetts-Amherst, Amherst, Massachusetts 01003, USA*

[c] *Department of Environmental, Earth and Ocean Sciences, University of Massachusetts, Boston, Boston, Massachusetts 02125, USA*

ABSTRACT

Floods cause environmental hazards and influence on socio-economic activities. In this study, we evaluated the historic flood frequency at a confluence in the middle Yellow River, China. A non-parametric, multivariate, empirical, orthogonal function matrix model, which consists of time correlation coefficients of flood discharge at different gauge stations and flood events was used for the analysis of flood frequency. The model addresses the characteristics of confluent floods such as frequency and the probability in multiple tributary rivers. Flood frequency analysis is often coupled with studies of hydrological routing processes that reduce the flood capacity of the rivers. Flood routing to the confluence were simulated using kinematic wave theory. Results of this flood frequency analysis showed that flooding frequency has intensified in the past 500 years, especially during the 19th century. Flooding in streams above the confluence was more frequent than in streams below the confluence. Over the last 2000 years, concurrent flooding in multiple tributary rivers accounted for 67.5% of the total flooding in the middle Yellow River. Simulation of flood routing processes shows that the decreased flooding capacity and elevated river bed of the shrunken main channel leads to an increased flood wave propagation time (24–52.3 h) in the study area after 1995. The model indicates that human activities, such as constructions of the Sanmenxia Dam, have changed flood routing boundary conditions and have contributed to the increased flood frequency at the confluence. Copyright © 2007 John Wiley & Sons, Ltd.

KEY WORDS: flood frequency evaluation; the middle Yellow River basin; flood routing; flood discharge

Received 28 September 2006; Accepted 5 October 2006

INTRODUCTION

Flooding is a substantial natural hazard and can have significant effects on the long-term economic growth of a region (Beven, 1997). Flooding by rivers has been studied extensively for years and in some rivers occurs almost annually, such as in the middle Yellow River (Yu and Lin, 1996). Disastrous floods in the years of 1662, 1819 and 1868 caused more than 230 thousand human deaths (Qian, 1992; Wang, 2004). The 26 August and 19 October 2003 flood in the Yellow River resulted in $430 million property losses, and affected about 563 000 people (Wang *et al.*, 2005). On average, the river bed was elevated about 0.12 m and flood discharge capacity decreased by 10–23 m^3/s after each event (above a baseline of 4500 m^3/s peak discharge in Tongguan) from 1957 to 2003 (Wang *et al.*, 2005). Over the past two decades, the middle Yellow River basin has experienced rapid socio-economic development and has become more densely populated. Therefore, future floods are likely to have greater impacts on the ecosystem and the socio-economic environment of the middle Yellow River.

Frequency analysis focuses on data collection and flood event interpretation; and the technique can be used to understand and predict flooding behaviour (Eagleson, 1972; Diaz-Granados *et al*., 1984; Costa, 1987; Stedinger and Baker, 1987; House and Pearthree, 1995; Sarka and Keith, 1997; Alcoverro *et al*., 1999; Yue *et al*., 1999; Cameron *et al*., 2000; Goel *et al*., 2000; Castellarina *et al*., 2001; Rico *et al*., 2000; Eric *et al*., 2004). Regional flood frequency analysis (RFFA) is an effective method (Castellarina *et al.,* 2001; Javelle *et al*., 2002) for obtaining flow

*Correspondence to: Yong Q. Tian, Department of Environmental, Earth and Ocean Sciences, University of Massachusetts at Boston, 100 Morrissey Blvd., Boston, MA 02125, USA. E-mail: yong.tian@umb.edu

statistics for ungauged sites using physiographic characteristics. RFFA can be used to estimate hydrological flow at sites where records are limited (Pandey and Nguyen, 1999). As summarized by Cunnane (1988) and Bobee *et al*. (1996), flood frequency analysis is often coupled with studies on routing procedures and hydrological processes. Models for describing flood routing processes are primarily physically based (Bathurst, 1986; Beven, 1987, 1997; HEC-RAS, 2002). Various modelling approaches have been successfully adopted to estimate flood peaks and volumes, such as bivariate normal distributions (Goel *et al*., 2000), multivariate Gaussian and exponential distributions (Singh and Krstanovic, 1987), the non-parametric multivariate kernel method (Moon and Lall, 1994) and the Gumbel distribution model (Todorovic, 1978).

However, characteristics of the different drainage systems affect flood frequency differently, in terms of both duration and intensity (Beven, 1997; Goel *et al*., 2000). In a large river basin, tributaries may distribute symmetrically or asymmetrically along the main channel. The influence of tributary floods to the water flow behaviours in main channel has not been well-studied. There is a need to develop modelling approaches for analyzing the possibility of concurrent floods of multiple tributaries and for improving our understanding of flood routing processes as well as the associated tributary drainage characteristics in a river basin.

Our study objective is to evaluate flood behaviours by considering flood frequency, concurrent floods of multiple tributary rivers, flood routing processes and associated impacts on regional ecological and socio-economic environments around rivers. First, we examined the historic flood series recorded in gauge data and then proposed a non-parametric multivariate empirical orthogonal function model, which includes time correlation coefficient of flood discharges. The model allows us to synthetically analyze flood frequency of the unusual drainage system in the middle Yellow River basin. The two components of the model are a spatial matrix and a temporal matrix. The spatial matrix represents the relationship of flood peak discharges or water levels at different sites. The temporal matrix represents the relationship between individual discharges or water levels in a series of flood events. Thus, the model describes both temporal and spatial characteristics of flood events. Second, we proposed a flood routing model based on rigorous kinematic wave propagation theory and simulated routing processes by using the characteristics in the middle Yellow River basin. The results from simulating two flood events provided useful quantitative information on hydrological processes that can be used for analyzing the causes of floods and the impact of environment change on flood characteristics.

STUDY AREA

Our study area is in the middle of Yellow River (between Hekou to Huanyuankou-Taohuayu) spanning from (35^0 N, 105^0 E) to (41^0 N, 1150 E,) as displayed in Figure 1. The site has a drainage area of 32 354 km^2, which accounts for 43% of the whole Yellow River watershed. The confluence area of the middle Yellow River network consists of the main river stream and its four tributaries, including Weihe River, Jinghe River, Luohe River and Fenhe River in the middle Yellow River.

The total annual precipitation in the study area ranges from 300 mm to 1000 mm. About 48% of the precipitation (145 mm–480 mm) occurs in the summer season (from July to August) in the form of rainstorms (rainfall amounts are over 50 mm in 24 h). These rainstorms are mostly of short duration and high intensity (Table I). There are three types of rainstorms: local rainstorm, broader-area rainstorm and continuous overcast rainstorm. Local rainstorms occur in all regions annually, but rarely form large floods. Whereas, a broader-area rainstorm or a continuous overcast rainstorm may easily lead to a disastrous flood. Historically, continuous overcast rainstorms accounted for 20% of the total rainfall events. For example, the rainfall on 27th May 1973 in Heiyukou (in Guanzhong Plain) reached 59 mm in just 5 min; a rainstorm on 1st August 1973, in Shilazhuohai (Luohe River) reached 1050 mm in 10 h; a 12-day continuous overcast rainstorm that started on 14th August 1981 in the west Guanzhong Plain reached a total precipitation of 930 mm.

Precipitation of the area recorded between 1930 and 1990 shows a fluctuating curve (Figure 2). A rainstorm covering the whole drainage area would most likely lead to a river flood. We selected six sites for observing flood events in each of five individual tributary rivers: Huaxian, Longmen, Tongguan, Xianyang, Zhangjiashan and Zhuangtou. We focused on these main tributary rivers in this study (Figure 1).

DOI: 10.1002/rra

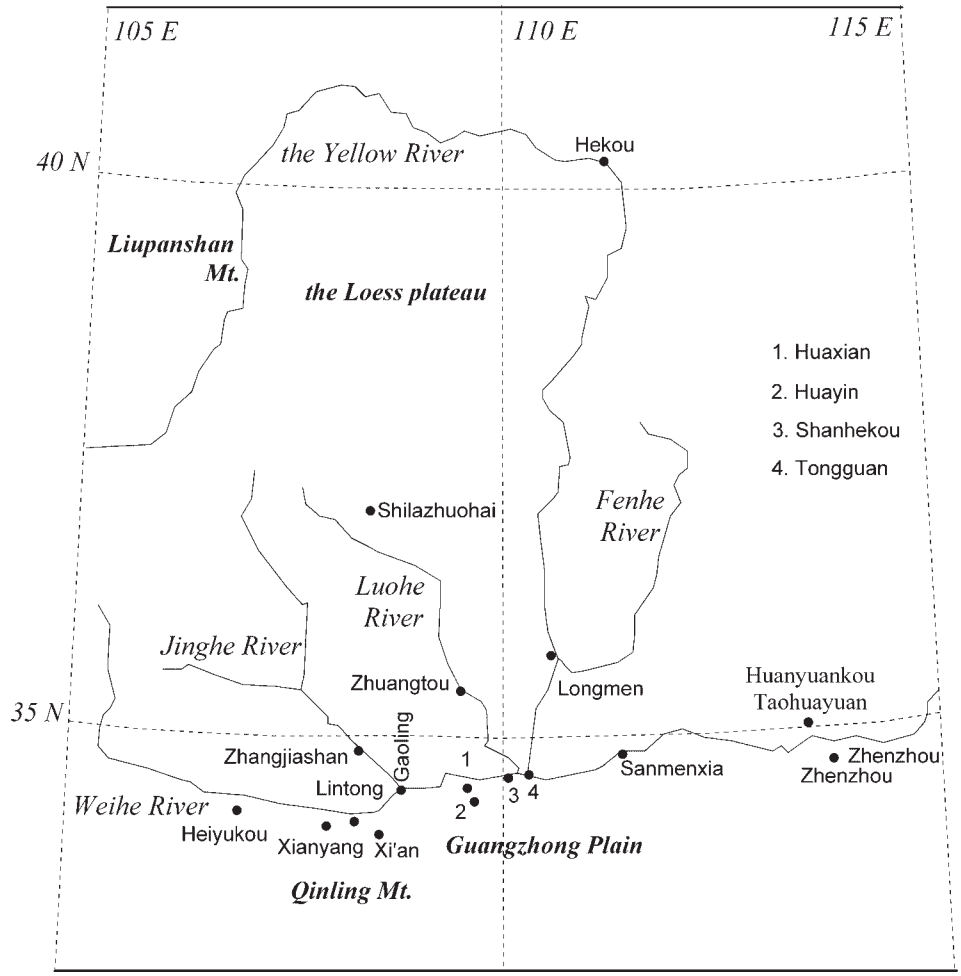

Figure 1. Sketch map of the middle Yellow River (From Hekou to Tongguan is called north main stream. Tongguan is the junction point of Weihe River and Yellow River. Fenhe River flows into Yellow River, Jinghe River flows into Weihe River at Gaoling and Luohe flows into Weihe River at Shanhekou. Distance from Shanhekou to Tongguan is 15 km and from Gaoling to Tongguan is 190 km)

MATERIALS AND METHODS

Data collection

Historic data has been increasingly used in recent years for estimating large flood events (Archer, 1987; Black and Burns, 2002; Williams and Archer, 2002). A catalogue of historic flood events (from 0 AD to 1949 AD) for the study area was compiled primarily from the archives of Systematic Research and Countermeasures for Huge Natural Disasters (China Disaster Prevention Committee, 1993), and using documents on China History Floods before 1990 (Huang, 1989). We extracted some useful information from references to the Climate of the Loess Plateau (Qiu, 1992) in the provincial chronicles archives (1470–1991). Gauge data (1950–2003) collected from the State Flood Control and Drought Relief Headquarters was used to improve the accuracy of the flood evaluation in the study area.

Flood series reconstruction

We evaluated the characteristics of documented historic floods by separating subjective and objective components. Objective verification refers to the historic and the scientific facts of flood events at the confluence,

DOI: 10.1002/rra

Table I. Rainstorms in the middle Yellow River Basin (from June to Sept 1981–2003)

Duration	Daily prep (mm)	Rainstorm type	Area
1981.08.09–10	60	Flood	W.R.
1981.08.14–16	127	Flood	L.R.& J.R.
1982.07.29–08.01	193	Flood	L.R., J.R. & M.Y.R
1983.09.07–08	139	Flood	J.R. & Y.R
1984.06.05–08	102	Non-flood	W.R.
1984.07.10–11	61	Flood	L.R.
1985.08.23–25	88	Flood	Y.R.
1986.07.09–10	78	Flood	W.R.
1986.09.08–09	82	Non-flood	W.R.
1987.06.21–22	64	Non-flood	Y.R.
1988.07.03–04	67	Non-flood	W.R.
1989.08.19–20	60	Flood	L.R. & J.R.
1990.08.10–16	97	Flood	L.R., J.R. & Y.R
1991.07.29–31	101	Non-flood	J.R. & Y.R
1992.09.17–19	89	Flood	W.R.
1993.07.05–08	105	Flood	L.R.
1994.07.10–11	61	Flood	Y.R.
1995.08.23–25	88	Non-flood	W.R.
1996.07.13–16	78	Flood	L.R., J.R. & Y.R
1997.07.21–22	78	Flood	W.R.
1998.07.03–04	64	Non-flood	Y.R.
1999.08.18–22	67	Flood	W.R.
2000.08.17–23	127	Flood	L.R. & J.R.
2001.07.21–27	93	Non-flood	W.R.
2002.07.25–31	89	Flood	J.R. & Y.R
2003.08.23–28	112	Flood	L.R, J.R & Y.R,W.R.

Y.R., Yellow River; W.R., Weihe River; L.R., Luohe River; J.R., Jinghe River.

such as levee debacle, bridge and construction damage, agriculture damage and livestock losses and other flood-related damages. We verified data using classification-indices (classifications such as huge flood, middle sized flood and small flood), statistical normalization and frequency analysis (such as *t*-test for dryness or wetness grades and 3-year moving average flood peak discharge). Historic records of flood events (Qian, 1992) were available back to 0 AD (centred on 1450–2003), whereas daily gauges were initiated in 1950. By comparing with the historic flood trends of European rivers, we reconstructed the characteristics of a long historic record series for the middle Yellow River basin.

Flood frequency analysis—correlation coefficient matrix

The frequency of large-scale flood events shows an increasing trend in the middle Yellow River basin (Qian, 1992; Yu and Lin, 1996; Wang, 2004). Flood frequency analysis has often been used previously in studying the trend of river floods (Beven, 1987; Macdonald and Werritty, 2001; Glaser and Stangl, 2003). Various indices [such as skewness coefficient, Monte Carlo experiments distribution functions of normal, three-parameter lognormal, Gumbel, Pearson Type 3, Weibull, Pareto and uniform)] have been introduced to monitor river floods on the basis of the regional flood characteristics (Cunnane, 1988; Bobee *et al.,* 1996; Burn, 1990, 1997; Jain and Lall, 2000; Jun-Haeng *et al*., 2001; Javelle *et al*., 2002; Palmer and Raisanen, 2002; Christensen and Christensen, 2003; Mudelsee *et al*., 2003). These flood indices are effective in relating flood dynamics to precipitation.

Simple correlation coefficients of flood discharges between rivers have been used to describe the frequency distribution of historic flood series. With gauge data, a non-parametric multivariate empirical orthogonal function model was used to address the relationship between flood events of rivers (Obled and Creutin, 1986; Rao and Hsieh,

DOI: 10.1002/rra

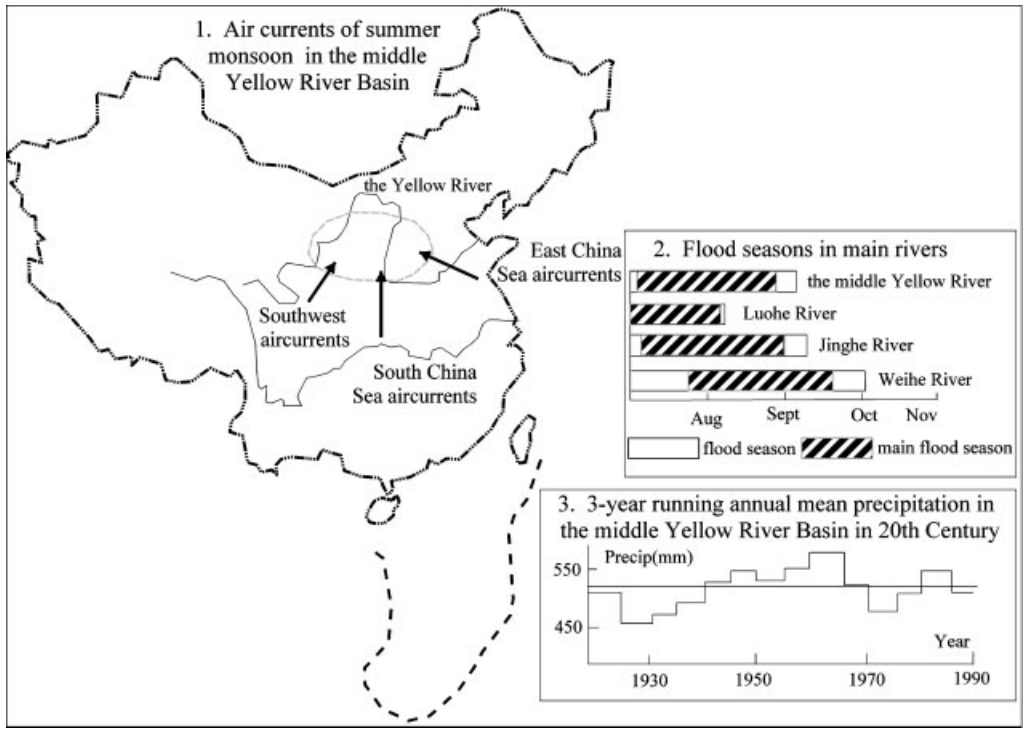

Figure 2. Climate situation in the middle Yellow River basin (1. Summer monsoon air currents transport routines; 2. Flood seasons of main rivers in study area; 3. 3-year running annual mean precipitation of middle Yellow River Bain in 20th century)

1991; Hisdal and Tveito, 1993; Loboda *et al*., 2005). We defined the flood time coefficient matrix (Θ) as the product of a spatial matrix and a temporal matrix. The spatial matrix ($\mathbf{X}$) represents the relationship between peak flood discharges or water levels at different sites. The temporal matrix ($\mathbf{F}$) represents the relationship between individual discharges or water levels in a flood series. If we use matrix Θ to represent the time coefficient of discharge Q at different stations and a series of flood events, then it can be computed by Equation (1) as below.

$$\Theta = \mathbf{X}'\mathbf{F} \tag{1}$$

The above equation represents interactive behaviours of flood discharge Q between spatial and temporal patterns. The two matrix variables $\mathbf{X}$ and $\mathbf{F}$ can be expressed as: $\mathbf{X} = \begin{bmatrix} X_1 \\ X_2 \\ X_3 \end{bmatrix}$

$$\mathbf{X} = \begin{bmatrix} X_1 \\ X_2 \\ X_3 \end{bmatrix} \tag{2}$$

where X_i is the eigenvector of the correlation coefficient matrix of flood discharge between gauge stations. This will be explained on the later of the section. To simplify, we explain the non-parametric multivariate empirical orthogonal modelling approach by using the flood events at the three discharge stations in our study site. Therefore, i ($1 <= i <= 3$) indicates the discharge stations: (1) Huaxian, (2) Zhuangtou and (3) Longmen.

$$\mathbf{F} = \begin{bmatrix} q_{1,1} & q_{1,2} & q_{1,3} & \cdots & q_{1,m} \\ q_{2,1} & q_{2,2} & q_{2,3} & \cdots & q_{2,m} \\ q_{3,1} & q_{3,2} & q_{3,3} & \cdots & q_{3,m} \end{bmatrix} \tag{3}$$

DOI: 10.1002/rra

where q_{ij} is the normalized discharge at station i in the flood event j ($1 <= j <= m$).

$$q_{ij} = \frac{Q_{ij} - \overline{Q}_i}{S_i} = \frac{Q_{ij} - \frac{1}{m}\sum_{j=1}^{m} Q_{ij}}{\sqrt{\frac{1}{m^2}\left(m\sum_{j=1}^{m} Q_{ij}^2 - \left(\sum_{j=1}^{m} Q_{ij}\right)^2\right)}} \tag{4}$$

where Q_{ij} is the maximum instantaneous hydrometric flood discharge at station i of flood event j. $\overline{Q_i}$ is the mean flood discharge at station i during m flood events. m is the maximum number of flood events considered in the study. S_i is the mean square of differences between the flood discharges at stations i in m flood events.

Suppose that R represents the time correlation coefficients matrix of flood discharges between gauge stations: Huaxian ($i = 1$), Zhuangtou ($i = 2$) and Longmen ($i = 3$). The element of R,r_{kh}, is derived from available historic flood events. Each individual element in the **R** matrix stands for the correlation coefficient of flood discharges between gauge station k ($1 <= k <= 3$) and station h ($1 <= h <= 3$).

Due to the symmetric features of the correlation coefficients between any two different stations, $r_{kh} = r_{hk}$ when $k <> h$ and $\forall k$, $h \in (1, 2, 3)$. Similarly, we have $r_{kh} = r_{hk} = 1$, when $k = h$, and $\forall k$, $h \in (1, 2, 3)$. For calculation purposes, we treat the matrix **R** as an asymmetric matrix. Therefore, **R** can be presented as,

$$\mathbf{R} = \begin{bmatrix} 1 & r_{1,2} & r_{1,3} \\ r_{2,1} & 1 & r_{2,3} \\ r_{3,1} & r_{3,2} & 1 \end{bmatrix} \tag{5}$$

As mentioned above, the spatial matrix (**X**) is the eigenvector of the matrix **R**. Its element, X_{i}, is a vector (x_{i1}, x_{i2}, x_{i3}), which represents the projective values of correlation coefficient elements, r_{i1},r_{i2} and r_{i3}. The eigenvector represents the independent relationship between elements in the matrix **R**. This relationship is necessary for the multiple combined equations.

Suppose T is the eigenvalue of the matrix **R**, **I** is the identity matrix and X_i is the eigenvector of the matrix **R**, then we have

$$|\mathbf{R} - T\mathbf{I}| = \begin{bmatrix} 1 - T & r_{1,2} & r_{1,3} \\ r_{2,1} & 1 - T & r_{2,3} \\ r_{3,1} & r_{3,1} & 1 - T \end{bmatrix} \tag{6}$$

By solving the above equation, we get three roots, T_1, T_2 and T_3. Therefore, we can calculate their eigenvectors (X_i) in Equation (7) by using each of their eigenvalues.

$$\mathbf{X} = \begin{bmatrix} X_1 \\ X_2 \\ X_3 \end{bmatrix} = \begin{bmatrix} x_{1,1} & r_{1,2} & r_{1,3} \\ r_{2,1} & r_{2,2} & r_{2,3} \\ r_{3,1} & r_{3,2} & r_{3,3} \end{bmatrix} \tag{7}$$

Based on matrix theory, for computation purpose, the relationship between matrix **R** and its eigenvalue T, eigenvector X can be expressed by the following equation:

$$|\mathbf{R} - T\mathbf{I}| \cdot |X| = 0 \tag{8}$$

then, we can get Equation (9) from Equations (5–8),

$$\begin{cases} (1 - T_i)X_1 + r_{1,2}X_2 + r_{1,3}X_3 = 0 \\ r_{2,1}X_1 + (1 - T_i)X_2 + r_{2,3}X_3 = 0 \\ r_{3,1}X_1 + r_{3,2}X_2 + (1 - T_i)X_3 = 0 \end{cases} \tag{9}$$

DOI: 10.1002/rra

From Equations (1–9), we get the time coefficient matrix (Θ) of flood discharge Q in station i

$$\Theta = [X_1\ X_2\ X_3] \cdot \begin{bmatrix} q_{1,1} & q_{1,2} & q_{1,3} & \cdots & q_{1,m} \\ q_{2,1} & q_{2,2} & q_{2,3} & \cdots & q_{2,m} \\ q_{3,1} & q_{3,2} & q_{3,3} & \cdots & q_{3,m} \end{bmatrix} \tag{10}$$

A higher absolute value of time coefficient (Θ) indicates a higher probability of confluence flood occurrence. By using the time correlation coefficient of flood discharges, this non-parametric multivariate empirical orthogonal function model improves preciseness of frequency analysis in the temporal and the spatial dimension.

Analysis of flood routing processes—Kinematic wave theory

Generally, there are two schemes for simulating flood evolution: a simplified scheme and a scheme that uses St. Vennant equations (Bathurst, 1986). The simplified scheme, which includes water level discharge, Muskingum-Cunge (Eric *et al*., 2004), instantaneous velocity of fluid flow and microwave scope theory, is a statistical method describing the characteristics of flood routing processes. The simplified scheme is an empirical approach and has no indication of physical process. The scheme that uses St. Vennant equations describes one-dimensional unsteady flow in wide rectangular channels expressed per unit channel width using equations of continuity and momentum. Because of the analytical features provided by the St. Vennant equations, we adapted this scheme for analyzing the flood routing processes.

There are two ways to solve the St. Vennant equations: (1) using characteristic discharge curves (t-x curve, which simply reveals the rainfall–flood relationship of discharge between the time-t and space-x planes) and (2) using kinematic wave theory (KW) (Beven, 1997; Keskin and Agiralioglu, 1997; Ren and Cheng, 2003; Eric *et al*., 2004). The Kinematic wave (KW) model has been described as an accurate approximation of the Saint-Venant shallow water equations governing one-dimensional unsteady free surface flows (Hager and Hager, 1985; Chung *et al*., 1993; Chalfen and Niewmiec, 1996; Ren and Cheng, 2003). Therefore, for this study, we adapted the kinematic wave theory approach to route flood flows through the main channel (from the confluence area to the Sanmenxia Dam) and to evaluate the propagation of flood wave, flood wave travel times and reduction in peak discharge (attenuation) of flood waves along the channel.

The processes of flood flow routing through main channel (q_{L}), the propagation of waves (B), flood wave travel times (t) and peak discharge (attenuation) of flood waves (Q) are described in this section. The lateral inflow per unit time per unit channel length (m^2/s), q_{L} was calculated with the equation of continuity (Costa, 1987):

$$\frac{\partial Q}{\partial x} + B\frac{\partial Z}{\partial t} = q_L \tag{11}$$

and based on the conservation of energy, we get the momentum equation as below (Ren and Cheng, 2003),

$$\frac{\partial Q}{\partial t} + 2v\frac{\partial Q}{\partial x} + (gA - BV^2)\frac{\partial Z}{\partial x} - V^2\frac{\partial A}{\partial x}\bigg|_z + g\frac{nQ|Q|}{AR_{\mathrm{h}}^{4/3}} = 0 \tag{12}$$

where, Q is flood discharge (m^3), x is the coordinate horizontal in flow direction, B is the velocity of propagation of the kinematic wave, Z is water level (m), t is the time (s), V is velocity (m/s); g is acceleration due to gravity ($\mathrm{m/s}^2$), A is cross-sectional area of the flow (m^2); R_{h} is the hydraulic radius (m).

The steady flow approach was used in the kinematic wave modelling in the determination of water levels, flow and stage. The steady flow was implemented by setting manning equation as the steady-state rating curve equation. However, flood flow will be mostly in unsteady manners because of attenuation effects and restrictions to flow. A steady flow model would be accurate in estimating peak flow. Such results can be overestimating the flow volume prior to peak flow. The steady-state predictions are realistic if the flow rate keeps constant long enough to fill all water storage. Assuming steady flow is acceptable in estimating hydro dynamic properties in the main channel, during a flooding from rainstorm, as the channel and flow conditions do not vary greatly. Using steady flow approach has the advantage in the computations in order to avoid oscillation in results.

DOI: 10.1002/rra

The friction slope S_f is approximated by Manning's equation,

$$S_f = \frac{n^2 V|V|}{y^{4/3}} \tag{13}$$

$$V = \frac{1}{n} R_h^{2/3} S_f^{1/2} \tag{14}$$

where S_f is the friction slope, n is the Manning's roughness coefficient, R_h is the hydraulic radius (m) and $V|V|$ replaces V^2 to account for the possibility of flow reversal.

We used the preissmann four-point implicit scheme to solve the channel flow equations and avoid the disturbing effect of the numerical diffusion on modelling results. As shown in Figure 3, the flow domain is divided into a number of flow reaches. Accordingly, for a point like 'p' located in a rectangular grid, the average values and derivatives are given by,

$$\frac{\partial f}{\partial x} \approx \frac{\theta(f_{i+1}^{j+1} - f_i^{j+1}) + (1-\theta)(f_{i+1}^{j} - f_i^{j})}{\Delta x_i} \tag{15}$$

$$\frac{\partial f}{\partial t} \approx \frac{f_{i+1}^{j+1} + f_i^{j+1} - f_i^{j} - f_{i+1}^{j})}{2\Delta t} \tag{16}$$

where f is the function of Q, Z, A, V. The subscript of f is the identity of different river reaches; the superscript of f depicts different time periods. θ is the time-weighting coefficient. Δx_i is the length of the ith reach in a river. On substituting the average values of Equations (11) and (12) for the appropriate items in Equations (15) and (16), the following equations are obtained:

$$\begin{aligned} -Q_{i-1}^{j+1} + Q_i^{j+1} + C_i Z_{i-1}^{j+1} + G_i Z_i^{j+1} &= D_i \\ E_i Q_{i-1}^{j+1} + G_i Q_i^{j+1} - F_i Z_{i-1}^{j+1} + F_i Z_i^{j+1} &= \varphi_i \end{aligned} \tag{17}$$

where,

$$\begin{aligned} C_i &= \frac{\Delta x_i B_{ij-1/2}}{2\theta\Delta t} \\ D_i &= \frac{1-\theta}{\theta}(Q_{i-1}^{j} - Q_i^{j}) + C_i(Z_{i-1}^{j} - Z_i^{j}) + \frac{\Delta x_i}{\theta} q_L \\ E_i &= \frac{\Delta x_i}{2\theta\Delta t} - 2V_{i-1/2}^{j} + \frac{g}{2\theta}\left(\frac{n^2}{R^{1.33}}\right)_i^j |V_{i-1}^{j}|\Delta x_i \\ F_i &= (gA - BV^2)_{i-1/2}^{j} \\ \varphi_i &= \frac{\Delta x_i}{2\theta\Delta t}(Q_{i-1}^{j} + Q_i^{j}) + \frac{2(1-\theta)}{\theta} V_{i-1/2}^{j}(Q_{i-1}^{j} + Q_i^{j}) + \frac{1-\theta}{\theta}(gA - BV^2)_{i-1/2}^{j}(Z_{i-1}^{j} - Z_i^{j}) + \frac{\Delta x_i}{\theta}(V^2 \frac{\partial A}{\partial x}\Big|_z)_{i-1/2}^{j} \end{aligned} \tag{18}$$

The approaching method was used to estimate flood influence on kinematic wave propagation based on upper boundary conditions of flood discharge. Suppose that a flood occurred in the cross-section i of the confluence area, the kinematic wave propagation approaching equation in cross-section kk is represented as,

$$Q_{kk} = P_{kk} + R_{kk} Z_{kk} \tag{19}$$

in the cross-section $(i-1)$,

$$Q_{i-1} = P_{i-1} + R_{i-1} Z_{i-1} \tag{20}$$

DOI: 10.1002/rra

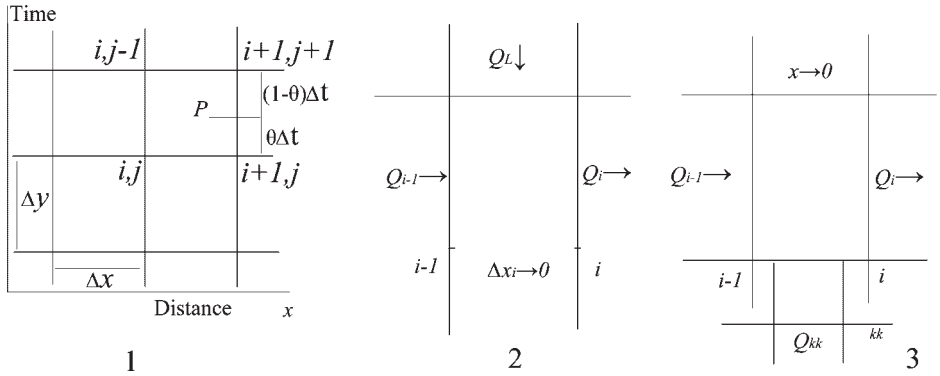

Figure 3. Four-point implicit finite difference scheme for Kinematic wave solution

and in the confluence cross-section, upper and lower boundaries conditions are represented as,

$$\begin{cases} Q_i = Q_{i-1} + Q_{kk} \\ Z_{i-1} = Z_i + Z_{kk} \end{cases} \tag{21}$$

therefore, the approaching equation for the cross-section *kk* may be written as,

$$\begin{cases} Z_{i-1} = Z_i \\ Q_i = (P_{i-1} - P_{kk}) + (R_{i-1} - R_{kk})Z_i \end{cases} \tag{22}$$

and the approaching coefficients,

$$\begin{cases} P_i = P_{i-1} + P_{kk} \\ R_i = R_{i-1} + R_{kk} \end{cases} \tag{23}$$

The variations of friction parameter n in Equation (18) increase in relation to the highest wave number. Such function might result in a wave speed greater than the reality. In these situations, it usually causes instabilities. This numerical scheme needs a dissipation mechanism in order to eliminate accumulation of dispersion errors. Therefore, it is advisable to increase the coefficient of time weighting parameter, θ. Time coefficient is usually defined as 0.3–0.65 depending on the situations of roughness coefficient. Considering the complex of land surface conditions in the middle Yellow River, we define θ as 0.6, and the roughness coefficient as 0.032. Distance step was defined according to the length of the river reaches. The distance steps in this study were 0.5–5.5 km for 25 reaches and 1.8–4.0 km for 20 reaches. By considering the propagation of flood flow discharge peak and water level, we selected time steps as $\Delta t = 1$ h.

Model calibration and validation was conducted by using two flood events in June 1996. One flood event was for calibrating model friction parameters and the other was for independent validation. Data used for calibration is the measurements in the reaches between Lintong and Huayin of the Weihe River. The results from calibration and validation confirmed that our model is capable of predicting flood extent well with only flood discharge data.

RESULTS

Probability analysis of historic floods at the confluence

Table II shows the flood occurrences at the confluence in the middle Yellow River contributed from at least two tributary rivers in the past 2000 years. The historic flood records show that the probability of flood events at the confluence increased between 1450 AD and 1949 AD. The probability of occurrences of confluent floods from two tributary rivers accounted for 67.5% of the total floods (one river: 439, two rivers: 214, total of above two rivers: 317, therefore, 214/317 = 0.675). According to the historic records, confluent flood events that had contributions concurrently from all four tributary rivers (Weihe River, Jinghe River, Luohe River and Fenhe River) occurred only

DOI: 10.1002/rra

Table II. Historic records of flood occurrence in the middle Yellow River Basin

River name	0 AD–1949 AD		1450 AD–1949 AD							
	Y.R.	W.R.	L.R.	J.R.	F.R.	Y.R.	W.R.	L.R.	J.R.	F.R.
Y.R	71	23	15	6	17	57	20	12	3	4
W.R.	—	91	17	7	6	—	71	17	6	9
L.R.	—	—	42	7	7	—		17	6	10
J.R.	—	—	—	24	12	—	—	—	19	10
F.R.	—	—	—	—	32	—	—	—	—	15
W.R.-L.R.	10	—	—	—	5	9	—	—	—	—
W.R.-J.R.	6	—	—	—	3	5	—	—	—	—
W.R.-F.R.	2	—	—	—	—	3	—	—	—	—
L.R.-J.R.	5	6	—	—		4	6	—	—	—
L.R.-F.R.	4	8	—	—	—	3	4	—	—	—
W.R.-L.R.-J.R.	4	—	—	—	—	3	—	—	—	—
W.R.-L.R.-F.R	1	—	—	—	—	2	—	—	—	—
W.R.-J.R.-F.R	2	—	—	—	—	1	—	—	—	—
L.R.-J.R.-F.R	1	—	—	—	—	2	—	—	—	—
W.R.-J.R.-L.R.-F.R.	3	1								

Y.R., Yellow River; W.R., Weihe River, L.R., Luohe River; J.R., Jinghe River; F.R., Fenghe River.

four times: 1436, 1662, 1819 and 1933 (Huang, 1989; Wu, 1991; Editor Department of Yellow River, 1991; Zuo, 1991; Wang, 2004).

The records also indicate the significant changes in flood frequencies (Figure 4). For example, there are three notable historic flood peaks: (1) around the 17th century, (2) between the late 18th century and the early 19th

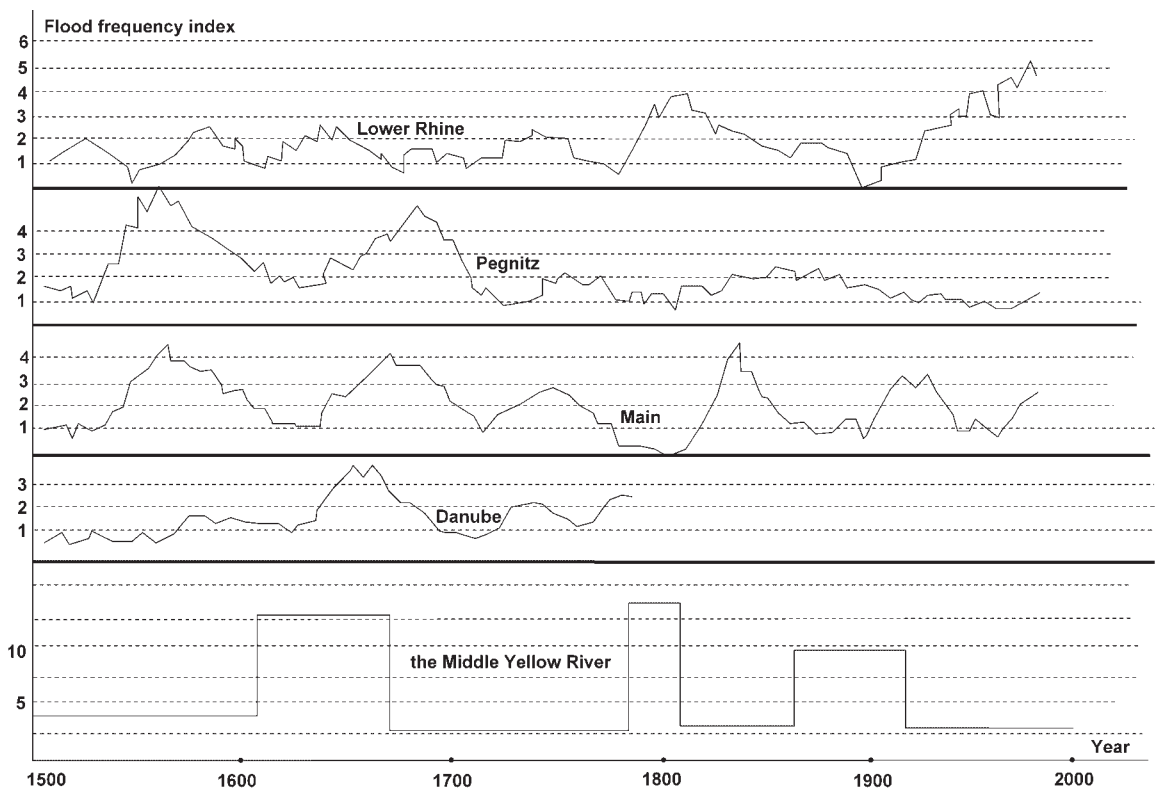

Figure 4. Historic flood frequencies between the Middle Yellow River and European rivers (revised after Glaser, R. and Stangl, H. 2003)

DOI: 10.1002/rra

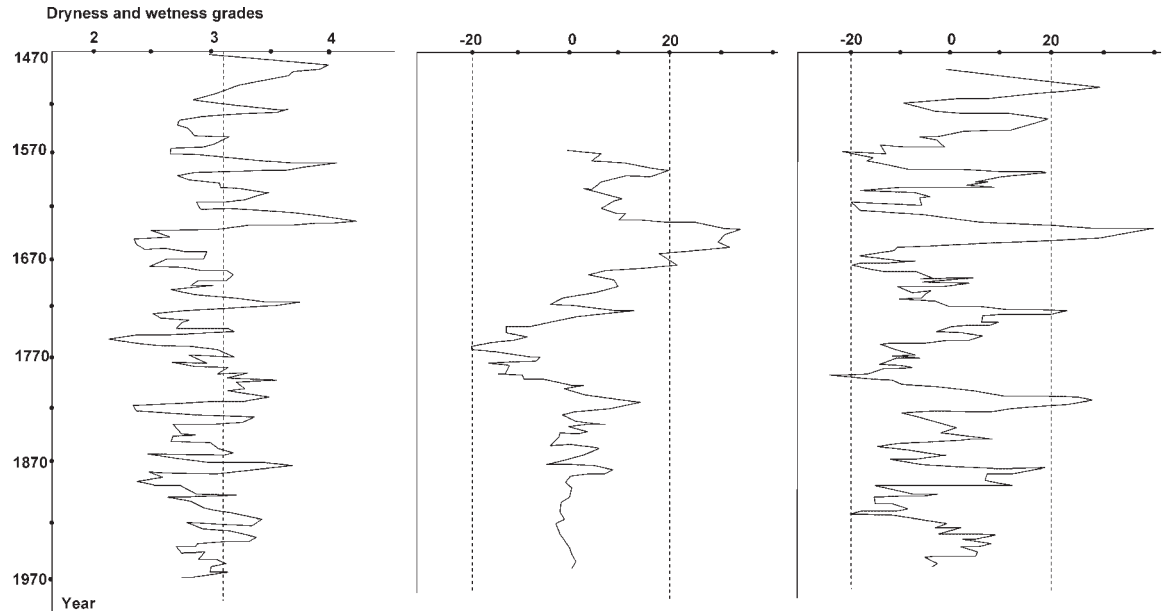

Figure 5. Running *T*-test for the dryness/wetness grades data in the middle Yellow River in summer (revised after Yu and Lin, 1996) (Drought grade value is above 3.24, normal value is between 3.24 and 2.90 and flood value is below 2.90. Left: series of 100-year running mean value. Middle: series of 20-year running mean value. Right: series of 10-year running mean value, vertical solid lines are mean values in the dryness/wetness periods, and dashed lines represent mean values of the century climate stages of the dryness/wetness)

century and (3) between the late 19th century and the early 20th century. Yu and Lin (1996) analyzed the abrupt changes of dry and wet climate of this study area for the last 522 years (1470–1991) (Figure 5). They rated the climate using three levels: wet, normal and dry. Their results showed different durations for the dry and wet periods. The average wet duration was 40 years with the average dry one being significantly shorter, 28 years. In the study period, there were only three wet periods, which accounted for 18% (94 years) of the total study period (522 years, 1470–1991). The century series indicated that there were two abrupt changes of 100-year scale in this region, around the 1650s (from drought to flood) and in the early l760s (from flood to normal). Overall, flood frequencies vary according to flood intensities at the confluence area in the middle Yellow River with larger floods occurring on a longer cycle. There was a 100-year cycle for severe floods ($\geq$27 400 m^3/s), a 33-year cycle for intensive floods ($\geq$24 100 m^3/s), a 23–26 year cycle for moderate floods ($\geq$19 600 m^3/s), a 10–12 year cycle for normal floods ($\geq$16 100 m^3/s) and a 3–5 year cycle for small floods ($\geq$14 300 m^3/s) during the past 2000 years.

According to the historic climate characteristics of the middle Yellow River basin, flood events occurred synchronously with wet climate. Almost 92.7% of flood events were in wet periods. The medium-term flood fluctuations in the middle Yellow River within the range of 30 to 100 years were quite similar to the flood occurrence in European rivers (Figure 4; Glaser and Stangl, 2003).

Modelling flood frequencies

Our modelling results successfully estimated the three huge flood events from 1950 to 2003. Integrated analysis of temporal and spatial characteristics of flood frequency was based on the non-parameters empirical function model. Table III shows the simulated results using the time coefficient of discharge model (equation 1) applied to the stations of Huaxian (Weihe River), Zhuangtou (Luohe River), Longmen (the middle Yellow River). The positive or negative values of the time coefficient of flood discharge describe the departures from the average. The higher absolute value means the higher probability of floods between rivers.

Modelled flood discharges for July (marked as Θ_7) matched the discharges in real flood events very well. For example, for the flood event from 27 July to 29 1966, the simulated Θ_7 was 4.37 and the normalized values of flood

DOI: 10.1002/rra

Table III. Simulated results from time coefficient of flood discharge model applied in stations of Huaxian (Weihe River) Zhuantou (Luohe River), Longmen (Yellow River)

	July				August			
	Huaxina	Zhuangtou	Longmen	Θ_7	Huaxina	Zhuangtou	Longmen	Θ_8
1950	1.4	−0.56	−0.25	0.28	−0.7	−0.46	−0.81	−0.1
1951	−0.69	−0.61	−0.49	−1.03	−0.87	−0.8	1.49	−0.01
1952	0	−0.63	−0.53	−0.69	1.3	−0.51	−0.95	−0.39
1953	1.06	−0.14	−0.82	0.07	0.13	3.26	1.89	3.42
1954	0.35	−0.66	2.13	0.87	3.18	0.09	0.19	1.5
1955	0.24	−0.51	−0.24	−0.32	−0.6	−0.53	−0.51	−0.98
1956	**1.6**	**2.39**	**0.28**	**2.58**	1.17	−0.23	−0.79	−0.14
1957	1.56	−0.35	0.18	0.73	−1.05	−0.39	−0.79	1.18
1958	0.69	0.64	1.45	1.55	2.24	−0.72	−0.05	1.39
1959	1.23	−0.21	1.92	1.54	0.39	0.57	0.95	1.13
1960	−0.57	−0.44	−1.13	−1.19	0.41	−0.05	−0.37	−0.39
1961	−0.02	−0.19	0.32	0.03	−0.65	−0.18	0.04	−0.37
1962	0.94	−0.45	−0.34	0.05	−0.38	−0.53	−0.61	−0.89
1963	−1.14	−0.52	−0.16	−1.05	−0.77	−0.85	−0.19	−1.01
1964	1.13	0.4	1.28	1.55	0.79	−0.14	2.3	1.61
1965	0.68	0.61	−0.68	0.44	−1.15	−0.94	−0.09	−1.78
1966	**2.2**	**3.85**	**1.25**	**4.37**	−0.5	0.66	0.49	0.54
1967	−0.36	−0.63	−0.66	−0.27	−0.9	0.14	**3.13**	**1.6**
1968	−1.3	−0.33	−0.09	−0.1	−0.13	0.69	−0.11	0.35
1969	−1.03	1	−0.88	0.54	−0.86	−0.72	−0.17	−0.95
1970	−0.66	−0.51	−1.19	−1.32	1.24	−0.42	1.51	1.14
1971	**−0.78**	**−0.49**	**2.48**	**0.53**	−0.48	0.97	−1.05	−0.17
1972	−1.01	−0.01	1.48	0.2	−0.99	−0.82	−0.93	−1.53
1973	−1.24	−0.32	−0.4	−1.1	1.56	0.34	−0.19	0.77
1974	−1.3	−0.43	0.53	−0.72	−0.65	−0.82	−0.44	−0.57
1975	0.1	2.24	−0.3	1.36	−0.89	−0.88	−0.43	−1.19
1976	−1.53	−0.63	−0.11	−1.31	1.57	0.14	0.8	1.23
1977	**1.66**	**3.45**	**2.54**	**4.48**	−0.44	0.44	1.47	1
1978	0.21	0.11	−0.55	−0.1	−0.97	1.23	−0.53	0.4
1979	−1.12	0.31	−1.06	−0.97	−0.86	0.5	1.33	0.78
1980	1.12	−0.54	−1.15	−0.33	0.35	−0.91	−1.18	−1.18
1981	0.69	−0.38	0.16	0.22	1.82	−0.59	−0.7	−0.07
1982	−1.05	−0.41	−0.24	−0.97	−0.34	−0.74	−0.8	−1.13
1983	0.66	−0.65	−0.66	−0.4	0.56	−0.8	−0.48	−0.6
1984	0.16	−0.54	−0.5	−0.52	0.39	−0.03	−0.27	−0.02
1985	−1.43	−0.43	−0.88	−1.53	−0.57	−0.24	−0.08	−0.45
1986	0.22	−0.62	−0.58	−0.59	−1.17	−0.92	−1.21	−1.85
1987	−0.84	−0.24	−1.35	−1.32	−0.26	−0.11	−0.02	−0.2
1988	0.21	−0.12	−0.36	−0.15	1.03	1.75	0.71	2.05
1989	−0.34	−0.33	0.6	−0.09	0.36	−0.94	−0.97	−1.07
1990	0.77	−0.27	−0.63	−0.98	−1	−0.86	−0.86	−1.52
1991	−0.12	−0.13	−0.34	−0.88	−0.52	−0.97	−1.27	−1.64
1992	−1.14	−0.33	−0.75	−1.23	1.02	3.95	0.11	3.18
1993	0.55	−0.63	−1.23	−0.74	−0.4	0.25	−0.59	−0.35
1994	−0.21	0.25	0.33	−0.12	−0.43	0.69	0.8	0.77
1995	−1.43	−0.54	0.59	−0.84	−0.44	0.29	−0.56	**0.32**
1996	0.87	−0.45	−1.44	−0.56	−0.51	0.26	**0.93**	**0.17**
1997	0.25	−0.4	−0.73	−0.39	0.21	−0.35	−0.31	−0.29
1998	0.12	0.17	−0.23	0.03	0.35	−0.48	0.34	−0.57
1999	−0.44	−0.35	0.56	0.25	0.48	−0.43	−0.42	−0.56
2000	0.24	−0.32	0.36	0.45	−0.37	0.45	0.39	−0.31
2001	1.03	0.45	1.52	1.45	−0.39	0.34	0.5	0.61
2002	0.48	0.69	−0.58	0.74	0.45	−0.74	−0.17	−0.67
2003	0.68	0.45	0.74	0.98	**2.65**	**3.75**	**3.24**	**4.58**

The bold type illustrates the significant years of simultaneous flooding in Middle Yellow River.

DOI: 10.1002/rra

discharges for Huaxian (HX), Zhuangtou (ZT) and Longmen (LM) were 2.20, 3.85 and 1.25. Corresponding to the modelled result, the gauged discharges reached 5180 m^3/s, 3360 m^3/s and 10100 m^3/s. For the flood event on 7 July 1977, the simulated Θ_7 was 4.48, and the normalized values of the flood discharges were 1.66, 3.45 and 2.54. The corresponding gauged discharges reached 3070 m^3/s, 4470 m^3/s and 14 500 m^3/s. In the above two flood events, the modelled Θ_7 values indicate high flood events. In reality, there were severe flood events. The model performance is consistent with other flooding years. Similarly, the low Θ_7 value stands for the low probability of floods at the confluence. For example, in the event of July 1971, the Θ_7 value was 0.53, and the normalized values of the flood discharge for the same three stations were -0.78, -0.49 and 2.48. The corresponding gauged discharges were 1280 m^3/s, 206 m^3/s and 14 300 m^3/s.

Based on our time coefficient model, we predicted flood events from 1996 to 2003. In July 2001, the Θ_7 value was 1.45, and the normalized values of flood discharge were 1.03, 0.45 and 1.52. In this scenario, a small flood event occurred at the confluence of the middle Yellow River, Weihe River and Jinghe River. In the events of 26th, 27th and 31st August 2003, the discharges reached 1140 m^3/s, 5100 m^3/s and 7230 m^3/s. The modelled flood discharge time coefficient in August (marked as Θ_8) was 4.58, and the normalized values of the flood discharges were 2.65, 3.75 and 3.24. In this scenario, there was a huge flood at the confluence of the middle Yellow River, Luohe River, Jinghe River and Weihe River. The simulation results using the non-parameters empirical function model with time coefficients revealed the relationship between flood probability and the true intensity of floods at the confluence.

Model results identified that the correlation coefficients of flood discharges between different stations are capable of describing the spatial distribution characteristics of flood frequency at the confluence. The spatial characteristics of flood frequency derived from the correlation coefficient analysis and *R*-squared values of the regression model (the methods of analyzing the relationship of flood discharges between stations) were compared to the documented historic flood events. Coefficient of variation (CV, ranging from 0 to 1) represents the variation degree of water-related variables in hydrology. The greater CV value means the higher probability of variation. The CV values of the annual flood discharges varied from 0.37–0.49 (Yellow River and Weihe River) to 0.89–0.98 (Jinghe River and Luohe River) (Table IV). Since the Fenhe River and Weihe River are tributaries of the middle Yellow River, and Jinhe and Luohe are tributaries of Weihe River, the values imply that the variation of the annual flood discharges was lower in the main streams than that in the tributaries. Meanwhile, records show that the duration of floods varied from 1 to 3 days in the main stream rivers at the confluence and from 5 to 7 days at the gauging stations in the tributaries. These phenomena were due to monsoon influences. In an earlier rainy season, flood may occur in the tributary several days before in the main stream so that effect of the tributary flood flow on the main stream is insignificant.

Modelling results (Table V) show that the correlation coefficients of flood discharges in the upper reaches were higher than the values downstream. For example, the correlation coefficient of flood discharge for the stream between Longmen and Tongguan was 0.67 and for the one between Xianyang and Huaxian was 0.78. The results also show that two nearer stations had a higher correlation coefficient value of flood discharges, for example the correlation coefficient in Tongguan between Yellow River, and Weihe River was higher than in Longmen between Weihe River and Luohe River. The correlation of the flood discharge was rather poor (0.05) between Zhangjiashan and Tongguan rivers because of the greater distance between the two stations. Also the floods in the single Jinghe River associated with the Zhangjiashan station had small effects on the Yellow River. Floods based on contributions from a greater number of tributary rivers would have more effects on behaviours of floods at their confluence areas, but have lower probability of co-occurrence. For example, probabilities of confluence floods of three tributary

Table IV. Coefficient of variation (CV) values in the middle Yellow River Basin

River name	Coefficient of variation of annual flood discharge
Main stream of Yellow river	0.37
Weihe river	0.49
Fenhe river	0.64
Jinghe river	0.89
Luohe river	0.98

DOI: 10.1002/rra

Table V. Correlation coefficient of flood discharge occurrence in the Middle Yellow River Basin

	The Yellow river		Weihe river		Jinghe river	Luohe river
	Longmen	Tongguan	Xianyang	Huaxian	Zhangjiashan	Zhuangtou
Longmen	1	0.67	0.15	0.21	0.16	0.07
Tongguan	—	1	0.17	0.29	0.05	0.20
Xianyang	—	—	1	0.78	0.36	0.11
Huaxian	—	—	—	1	0.58	0.13
Zhangjiashan	10	—	—	—	1	0.50
Zhuangtou	6	—	—	—	—	1
Weihe river						
Jinghe river	—	0.65	—	—	—	0.75
Weihe river						
Luohe river	—	0.63	—	—	—	—
Jinghe river						
Luohe river	—	0.55	—	—	—	—
Weihe river	—	0.50	—	—	—	—
Jinghe river						
Luohe river						

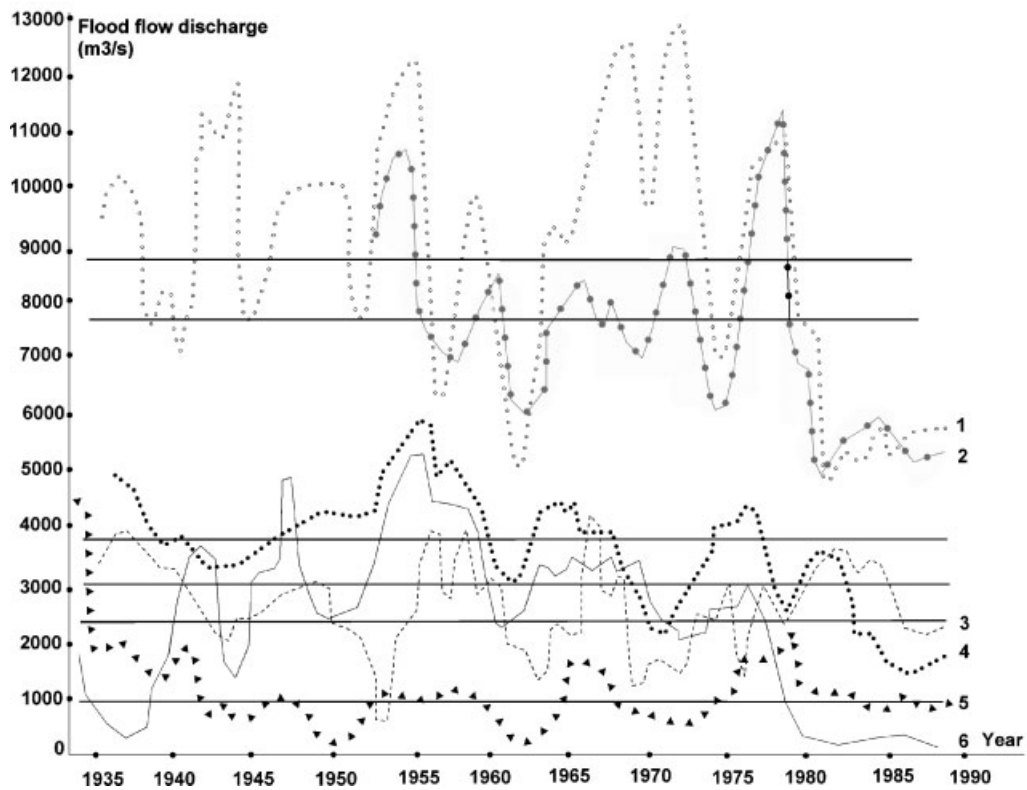

Figure 6. 3-year moving average flood peak discharge in middle Yellow River (1. Longmen, 2. Tongguan, 3. Xianyang, 4. Huaxian, 5. Zhangjiashan, 6. Zhuangtou)

DOI: 10.1002/rra

rivers were lower than that of two rivers, but higher than that of four rivers. The analysis showed that flood discharges at the two stations (Tongguan, in Yellow River and Huaxian, in Weihe River) had the highest correlation coefficient values. The next high coefficient was for the rivers: Weihe, Luohe and Jinghe. The lowest coefficients of flood discharge were from the segments: Yellow River, Jinghe River and Luohe River.

Using a 3-year moving average method for periodicity analysis (Figure 6) shows that high flood discharges were observed at the six sites (Huaxian, Longmen, Tongguan, Xianyang, Zhangjiashan and Zhuangtou) in 1935–1937, 1941–1944, 1952–1955, 1963–1973 and 1975–1979. The years with low flood discharge were 1937–1941, 1959–1963 and 1971–1991. Flood discharges varied from 1930 to 1990, and flood frequency at the confluence near Tongguan intensified during the past 30 years (Figure 6). This result demonstrated that the probability of flood occurrences at the confluence increased after 1970, when severe floods occurred almost every 2–6 years (e.g. big floods in 1971, 1977, 1979 and 1988, 1992, 1994, 1996 and 2003).

Degraded river channel conditions changed flood wave propagation

Results from using the kinematic wave theory (KW) and the defined parameters for flood routing processes from tributaries to the confluence showed that computed water levels or discharges generally agreed with the field measurements. We identified agreement by comparing the simulated results with the measured hydrographs at flood peak discharges and water levels from 6 June 1996 (Table VI). The simulated and measured hydrographs of flood discharge and water level from 2003 were also compared for the middle Yellow River and the comparison results are displayed in Figure 7. The most observed peak rainfalls at gauges exceeded the maximum within the past 10 years. Flood peak discharges in Zhangjiashan, Xianyang, Lintong and Huaxian were 4010 m^3/s, 5340 m^3/s, 5100 m^3/s and 3570 m^3/s. Total flood flows in Zhangjiashan, Xianyang and Huaxian discharged 1.25 billion cubic meters, 3.45 billion cubic meters and 6.26 billion cubic meters.

The flood routing analysis demonstrated that the situation of degraded river channels delayed flood wave propagation. For example, the water levels in Lingtong and Huaxian increased by 0.5 m and 1.2 m but the flood discharge decreased by about 64 m^3/s on average. The analysis showed that the flood wave propagation time was 24–52.3 h in 82.2 km from Lingtong to Huaxian in 1996 and 2003. This flood wave propagation time increased significantly in comparison to the propagation time of earlier events: 7 h in July 1977, 11 h in August 1981, 11–16 h, from 1985 to 1995. The increasing flood wave propagation times suggest that floodplains were probably inundated and flood routing channel roughness increased. These routing channel changes were more severe at the confluence areas (Figure 8). River channels were likely degraded by the silted and elevated river bed, and by the occupied floodplains of civilian construction projects. The shrunken main channels lead to decreasing flood capacity. The lower reaches were continuously silted for years, which shrank the main channel and reduced flood capacity.

DISCUSSION

Our study shows that disastrous floods in the study area were more frequent in the 19th century, but flood frequency has intensified over the past 30 years. The shortened flood intervals are generally correlated with fluctuating rainfall

Table VI. Observed and simulated peak discharge and water levels on 6 June 1996

	Zhangjiashan	Xianyang	Lintong	Huaxian	Tongguan
Water level (m)					
Observed	329.32	385.66	354.21	339.32	344.21
Computed	330.43	385.52	354.18	339.43	350.18
Absolute error	−1.11	0.14	0.03	−0.11	−5.97
Discharge (m3/s)					
Observed	427	469	640	627	470
Computed	424.5	467.88	634.15	621.58	464.5
Absolute error	2.5	1.12	5.85	5.42	5.5

DOI: 10.1002/rra

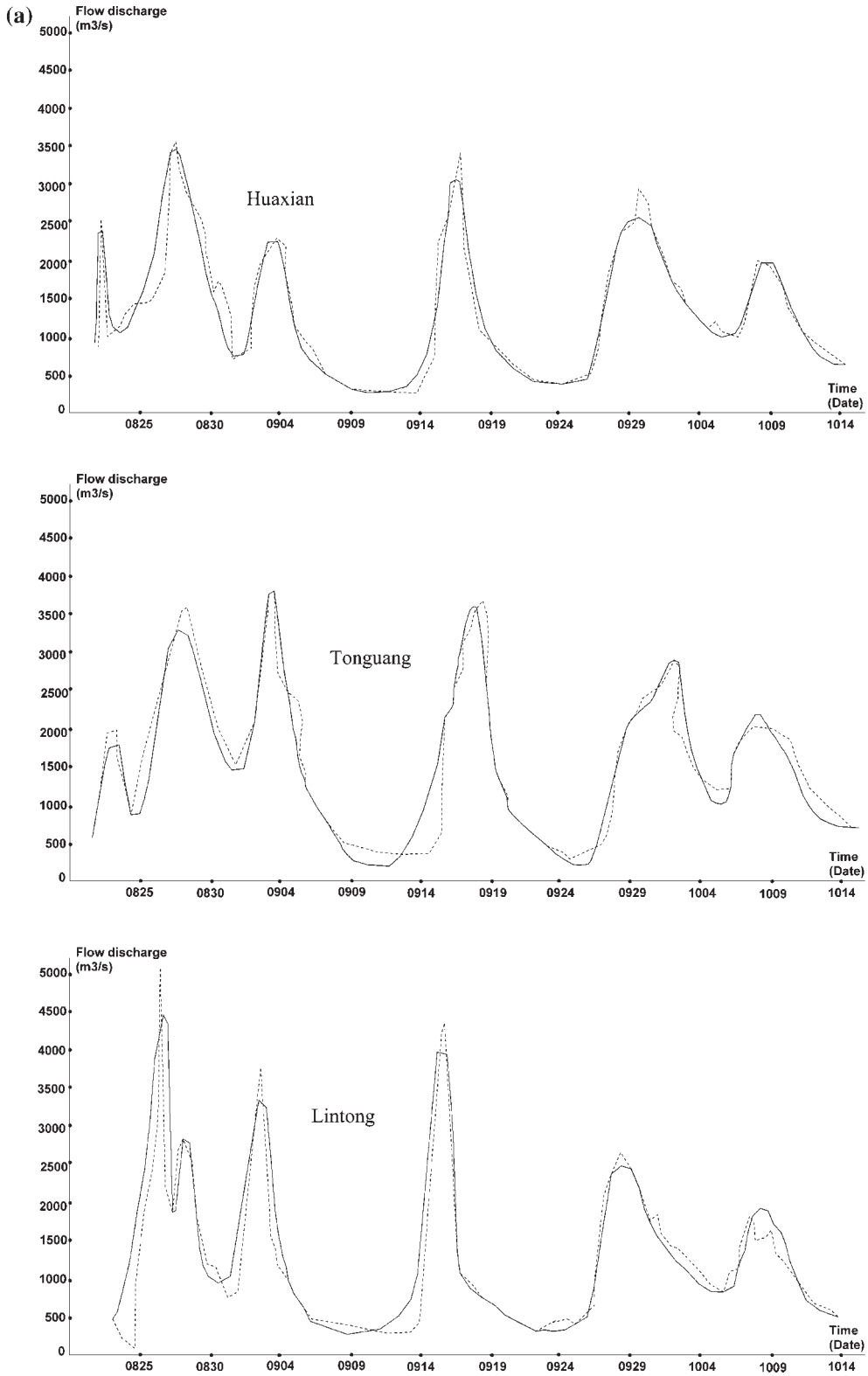

Figure 7. Simulated hydrographs of discharges (a) and water levels (b) at gauges in middle Yellow River in 2003 (25 August–20 October)

DOI: 10.1002/rra

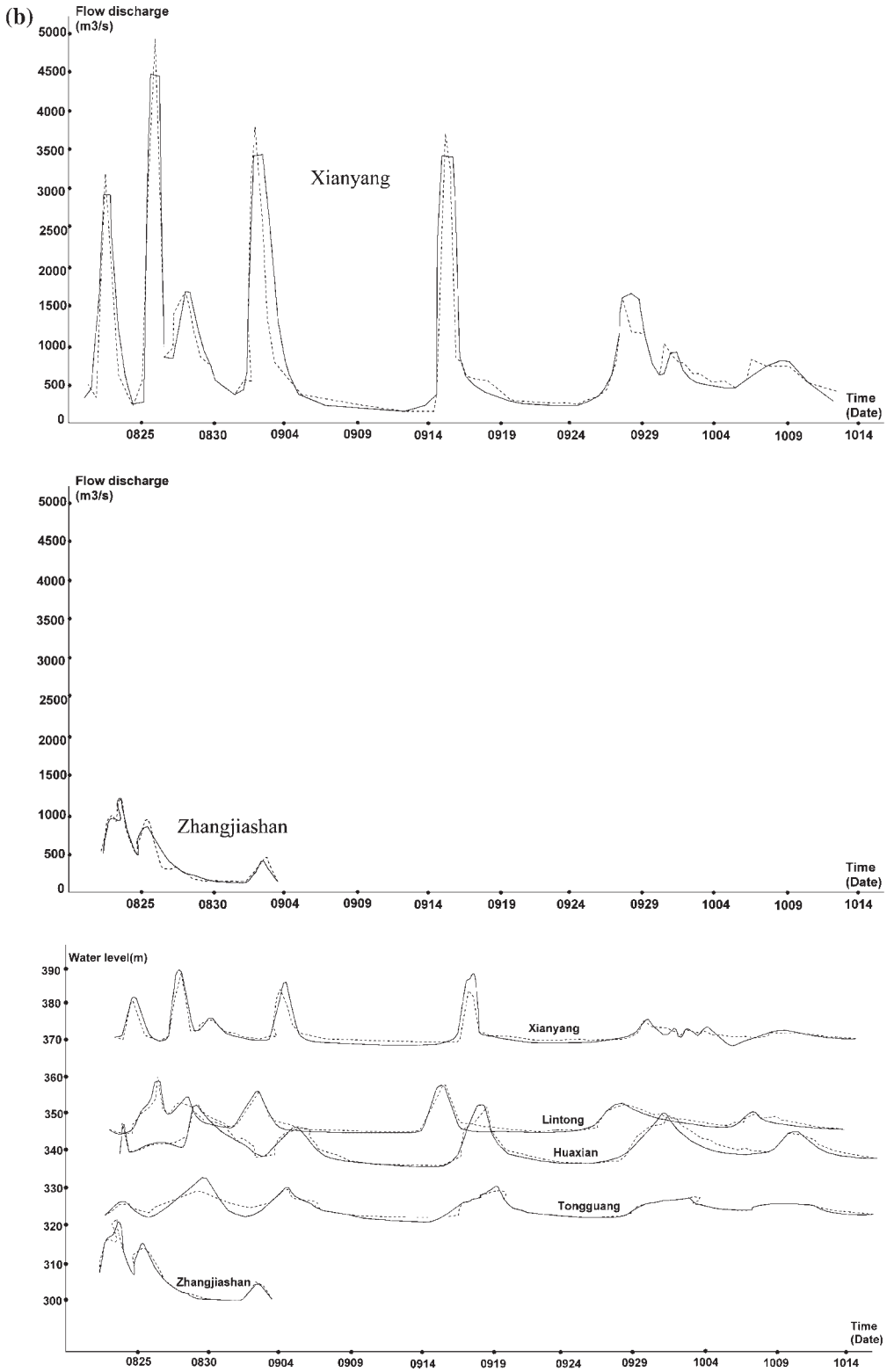

Figure 7. (Continued).

DOI: 10.1002/rra

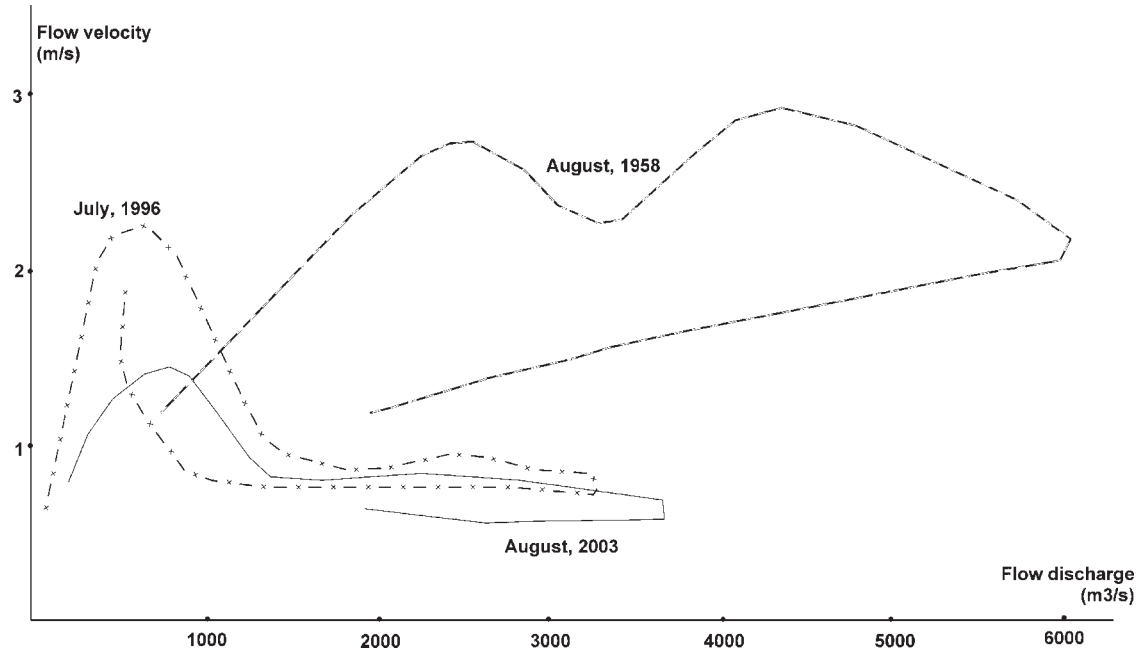

Figure 8. Relation between flood wave propagation velocity and discharge in Huaxian

and rising regional temperature. In addition to the climatic variables, the increased flood frequency was most likely also due to riverbed morphological change resulting from periodic flooding and sedimentation. The high correlation between rainstorms and flood occurrences suggest that climate change has and will continue to affect flood intensity and frequency. This suggestion from analyzing the flood frequency for the middle of Yellow River is consistent with world-wide evidences, such as results from the study conducted by Ludwig *et al.* (2004) for the Tet River (Southern France). Based on the studies by Yu and Neill (1993), high intensity rainfall could occur more frequently in a CO_2-warmed world. If results from Yu and Neill (1993) can be applicable to our study area, then global temperature increases tend to lead to more high intensity rainfall. Therefore, the influence of climate change must be considered in long-term planning for flood management schemes.

The correlation coefficient of flood discharges derived from the historic flood records were effective in predicting the flood events from 1996 to 2003. Correlation coefficients of flood discharges in upper reaches were found to be higher than those in lower reaches and also the proximity of gauging stations lead to higher correlation coefficient values. Therefore, carefully linking multiple water level measurements could be effective in predicting future trends of flood frequency.

Since Kinematic Wave theory model is affected by upper boundary conditions of flood discharge, human activities do alter the upper boundary conditions of rivers so that would be indirect factors for estimating flood propagation waves and description of flood routing processes. Exemplary human activities changing upper boundary conditions of flood discharges are construction of Sanmenxia Dam, aggravate potential confluent flood disasters, and change flood routing boundary conditions contributing to flood occurrence. This believes is supported by that urban development (channel form and streambed disturbance) has impact on interannual streamflow patterns reported by Konrad *et al.* (2005). Land use changes and construction activities have impacts on flood propagation waves and flood routing processes by increasing soil erosion and leading to declined flood capacity and elevated river bed of a shrunken main channel. The high sediment load of the river is one of the reasons that flood wave propagation times increased (to 24–52.3 h) in the study area after 1995. The river channels were unilaterally dominated by silting with litter deposits being flushed out and the silting central region moved upstream continuously. The annual sediment load of 1.6 billion tons carried by the Yellow River (the records in 1919–1985)

DOI: 10.1002/rra

can fill up any large reservoir in the world very quickly. Therefore, using reservoirs to control floods and regulate flows on the Yellow River has proved to be difficult.

In 1955, the government approved an ambitious plan of Yellow River management (ISP, YRCC, 1991). The plan aimed to put the river completely under control, eliminating the flood and drought disasters in the basin, stopping the water and soil losses on the Loess Plateau, and making the best use of the water resources for irrigation, electricity generation and navigation. Yet the soil loss was not alleviated as expected. Until 1979, the controls on soil losses were in place only for an area of 75.7 thousand km^2, or 40% of the planned area. As a result, serious sediment filling problems appeared in some of the completed reservoirs. Two of the reservoirs were built on the lower Yellow River and functioned for 5 years. They had to be destroyed in 1963 due to serious sediment filling and the resulting higher water level. Sanmenxia Reservoir had a capacity of 35.4 billion m^3 and was the largest in China when it was finished in 1960. Yet the sediment accumulation in the reservoir was so high that the total volume of deposits in the section from Tongguan to the dam reached 3.65 billion cubic metres in the first 4 years. Since the reservoir raised the water level at Tongguan where the Weihe River joins the Yellow River, heavy siltation and flooding took place in the Weihe River. The Weihe River flood events caused colossal harm to residents in the tributary's basin. Thus the flow regulation pattern of the reservoir had to be changed by impounding both water and sediment during 1960–1964, through deterring flood and discharging sediment during 1964–1973, and storing clear water and releasing muddy flow after 1973.

The reservoir was modified twice to enlarge its release capacity for the implementation of a regulation pattern transform. The originally designed normal high-level had to be lowered from 350 m to 335 m above sea level so that the storage capacity could be enlarged from 35.4 billion m^3 to 9.64 billion m^3. Even though the average water level of the reservoir was kept in the range of 314–318 m above sea level after 1974, the water level at Tongguan was still kept at around 327.5 m above sea level, 3.8 m higher than that before the dam construction. Therefore the huge volume of sediment carried by the river prevents the full use of the valuable capacity of reservoirs to regulate the river as needed.

Another environmental problem is civilian construction projects occupying floodplains. This practice will lead to for an increased risk for potential confluent flood disasters. Almost one-third of the floodplains in the middle Yellow River were occupied by business markets, factories and residential houses, and two-third of the floodplains were cultivated as farming lands. On one hand, these occupied floodplains are most likely to hold back flood flow and raised water levels at the confluence. On the other hand, a large loss of property and life is inevitable when heavy flooding occurs.

CONCLUSION

In this study, historic flooding events at the confluence of the middle Yellow River were evaluated to study the trend of flood frequency, intensity and probability of co-occurrence of floods from multiple tributaries (State Flood Control and Drought Relief Headquarters, 1992). In referencing to historic data, the non-parametric, orthogonal function matrix model introduced in the study was examined to be appropriate for analyzing flood frequency. Also our Kinematic Wave theory model has improved the prediction of flood propagation waves and the understanding of flood routing processes.

Through the characteristics of confluent floods, it improved our understanding the changes of flood frequency, intensity and duration in the middle Yellow River. The model simulation confirmed that human activities such as constructions of the Sanmenxia Dam, have significant effects on flood characteristics due to the change of flood routing boundary conditions. The need of model improvement is on parametres calibration to deal with the uncertainty in flow in the river channel because of the intense exchange of sediment load on riverbeds and banks.

ACKNOWLEDGEMENTS

The study was partially supported grants of EU-SINO (ICA4–CT-2002-10004), the Chinese Academy of Sciences (KZCX3-SW-146), State Key Laboratory of Loess and Quaternary Geology (SKLLQG0417).

DOI: 10.1002/rra

REFERENCES

Alcoverro J, Corominas J, Gomez M. 1999. The barranco de Aras flood of 7 August 1996 (Biescas, Central Pyrenees, Spain). *Engineering Geology* **51**: 237–255.

Archer D. 1987. Improvement in flood estimates using historical flood information on the River Wear at Durham. *British Hydrological Society Symposium.*

Bathurst JC. 1986. Physically-based distributed modeling of an upland catchment using the Systeme Hydrologique Europeen. *Journal of Hydrology* **87**: 79–102.

Beven KJ. 1987. Towards the use of catchment geomorphology in flood frequency predictions. *Earth Surface Processes and Landforms* **12**: 69–82.

Beven KJ. 1997. TOPMODEL: a critique. *Hydrological Processes* **11**(9): 1069–1086.

Black AR, Burns JC. 2002. Re-assessing flood risk in Scotland. *Science of the Total Environment* **294**: 169–184.

Bobee B, Mathier L, Perron H, Trudel P, Rasmussen PF, Cavadias G, Bernier J, Nguyen VTV, Pandey G, Ashkar F, Ouarda TBMJ, Adamowski K, Alila Y, Daviau JL, Gingras D, Liang GC, Rousselle J, Birikundavyi S, RibeiroCorrea J, Roy R, Pilon PJ. 1996. Presentation and review of some methods for regional flood frequency analysis. *Journal of Hydrology* **186**: 63–84.

Burn DH. 1990. Evaluation of regional flood frequency analysis with a region of influence approach. *Water Resources Research* **26**(10): 2257–2265.

Burn DH. 1997. Catchment similarity for regional flood frequency analysis using seasonality measures. *Journal of Hydrology* **202**: 212–230.

Cameron D, Beven L, Tawn J, Nader P. 2000. Flood frequency estimation by continuous simulation (with likelihood based uncertainty estimation). *Hydrology and Earth System Sciences* **4**(1): 23–24.

Castellarina A, Burnb DH, Brath A. 2001. Assessing the effectiveness of hydrological similarity measures for flood frequency analysis. *Journal of Hydrology* **241**: 270–285.

Chalfen M, Niewmiec A. 1996. Analytical and Numerical Solution of Saint-Venant Equations. *Journal of Hydrology* **86**: 1–13.

Christensen JH, Christensen OB. 2003. Severe summertime flooding in Europe. *Nature* **421**: 805–806.

Chung W, Aldama AA, Smith JA. 1993. On the effects of downstream boundary conditions on diffusive flood routing. *Advance in Water Resources* **19**: 259–275.

Costa JE. 1987. Hydraulics and basin morphometry of the largest flash floods in the conterminous United States. *Journal of Hydrology* **93**: 313–338.

Cunnane C. 1988. Methods and merits of regional flood frequency analysis. *Journal of Hydrology* **100**: 269–290.

Diaz-Granados MA, Valdes JB, Bras RL. 1984. A physically based flood frequency distribution. *Water Resource Research* **20**(7): 995–1002.

Eagleson PS. 1972. Dynamics of flood frequency. *Water Resource Research* **8**(4): 878–898.

Editorial Department of Yellow River. 1991. *Yellow River Records—Flood Defense, Henan People*. Publishing House: Zhenzhou; 117–231.

Eric G, Marc L, Michel D. 2004. Hydrological analysis of the river Aude, France, flash flood on 12 and 13 November 1999. *Journal of Hydrology* **286**: 135–154.

Glaser R, Stangl H. 2003. Historical floods in the Dutch Rhine Delta. *Natural Hazards and Earth System Sciences* **3**: 1–9.

Goel NK, Kurothe RS, Mathur BS, Vogel RM. 2000. A derived flood frequency distribution for correlated rainfall intensity and duration. *Journal of Hydrology* **288**: 56–67.

Hager WH, Hager K. 1985. Application limits for the kinematic wave approximation. *Nordic Hydrology* **16**: 203–212.

HEC-RAS. Hydraulic Reference Manual, Version 3.1 November 2002. available for download at www.hec.usace.army.mil.

Hisdal H, Tveito OE. 1993. Extension of runoff series by the use of empirical orthogonal functions. *Hydrology Science Journal* **38**: 33–50.

House PK, Pearthree PA. 1995. A geomorphologic and hydrologic evaluation of an extraordinary flood discharge estimate: Bronco Creek, Arizona. *Water Resources Research* **31**(12): 3059–3073.

Huang MS. 1989. *China History Floods (Upper Volume)*. Cathay Bookshop Publishing House: Beijing; 120–135.

ISP, YRCC (Institute of Survey and Planning, Yellow River Conservancy Commission). 1991. *Annals of planning theYellow River (in Chinese)*. Henan People's Press: Zhengzhou; 112–154.

Jain S, Lall U. 2000. The magnitude and timing of annual maximum floods: trends and large-scale climatic associations for the Blacksmith Fork River, Utah. *Water Resources Research* 3641–3652, 36, 12.

Javelle P, Ouarda TBMJ, Lang M, Bobee B, Galea G, Gresillon JM. 2002. Development of regional flood-duration-frequency curves based on the index-flood method. *Journal of Hydrology* **258**: 249–259.

Jun-Haeng H, Boes DC, Salas JD. 2001. Regional food frequency analysis based on a Weibull model: Part 1, Estimation and asymptotic variances. *Journal of Hydrology* **242**: 157–170.

Keskin ME, Agiralioglu N. 1997. A simplified dynamic model for flood routing in rectangular channels. *Journal of Hydrology* **202**: 320–314.

Konrad CP, Booth DB, Burges SJ. 2005. Effects of urban development in the Puget Lowland, Washington, on interannual streamflow patterns: Consequences for channel form and streambed disturbance. *Water Resources Research* **41**(7): Art. No. W07009.

Loboda NS, Glushkov AV, Khokhlov VN. 2005. Using meteorological data for reconstruction of annual runoff series over an ungauged area: Empirical orthogonal function approach to Moldova-Southwest Ukraine region. *Atmospheric Research* **77**(1–4): 100–113.

Ludwig W, Serrat P, Cesmat L, Garcia-Esteves J. 2004. Evaluating the impact of the recent temperature increase on the hydrology of the Tet River (Southern France). *Journal of Hydrology* **289**(1–4): 204–221.

Macdonald AR, Werritty BA. 2001. Historical and pooled flood frequency analysis for river Ouse, York, UK, http://www.nwl.ac.cn/hec/seclected papers/floods.html.

Mingshi H. 1989. *China History Floods (Upper Volume)*. Cathay Bookshop Publishing House: Beijing; 120–135.

DOI: 10.1002/rra

Moon YI, Lall U. 1994. Kernel quantile function estimator for flood frequency-analysis. *Water Resources Research* **30**(11): 3095–3103.
Mudelsee M, Borngen M, Tetzlaff G, Grunewald U. 2003. No upward trends in the occurrence of extreme floods in central Europe. *Nature* **425**: 166–169.
Obled Ch, Creutin JD. 1986. Some developments in the use of empirical orthogonal functions for mapping meteorological fields. *Journal of Applied Meteorology* **25**: 1189–1204.
Palmer TN, Raisanen J. 2002. Quantifying the risk of extreme seasonal rainfall events in a changing climate. *Nature* **415**: 512–514.
Pandey GR, Nguyen VTV. 1999. A comparative study of regression based methods in regional flood frequency analysis. *Journal of Hydrology* **225**: 92–101.
Qiu LQ. 1992. *Climate of the Loess Plateau*. China Meteorological Press: Beijing; 213–256.
Rao A, Hsieh CH. 1991. Estimation of variables at ungauged locations by Empirical Orthogonal Functions. *Journal of Hydrology* **123**: 51–67.
Ren X, Cheng J. 2003. *River Hydrology*. Hohai University Press: Nanjing; 110–143.
Rico M, Benito G, Barnolas A. 2000. Combined paleoflood and rainfall-runoff assessment of mountain floods (Spanish Pyrenees). *Journal of Hydrology* **245**: 59–72.
Sarka B, Keith B. 1997. Flood frequency prediction for data limited catchments in theCzech Republic using a stochastic rainfall model and TOPMODEL. *Journal of Hydrology* **195**: 256–278.
Singh VP, Krstanovic PF. 1987. A stochastic-model for sediment yield using the principle of maximum-entropy. *Water Resources Research* **23**(5): 781–793.
State Flood Control and Drought Relief Headquarters. 1992. *Flood Control Handbook*. China Science Press: Beijing; 230–256.
Stedinger JR, Baker VR. 1987. Surface water hydrology: historical and paleoflood information. *Review of Geophysics* **25**(2): 119–124.
Todorovic P. 1978. Stochastic-Models of Floods. *Water Resources Research* **14**(2): 345–356.
Wang X. 2004. The research on the flood peak flow forecast of Jiaokou in flood season. *Journal of Northwest Hydroelectric* **20**(3): 62–64.
Wang X, Du J, Wu M, *et al*. 2005. Situation analysis of rain, water and disaster for catastrophic flood in lower reaches of Weihe River in August, 2003. *Journal of Natural Disasters* **14**(3): 44–50.
Williams A, Archer D. 2002. The use of historical flood information in the English Midlands to improve risk assessment. *Hydrological Sciences Journal* **47**(1): 67–76.
Wu X. 1991. *Selected Works for Environment Change and Water-sand Dynamic Law Research* (Vol. 2). China Geology Press: Beijing; 132–234.
Yu B, Neill DT. 1993. Long-term variations in regional rainfall in the south-west of western-Australia and the difference between average and high-intensity rainfalls. *International Journal of Climatology* **13**(1): 77–88.
Yu S, Lin X. 1996. Abrupt change of drought/flood for the last 522 years in the middle reaches of Yellow. *Quarterly Journal of Applied Meteorology* **7**(1): 89–95.
Yue S, Ouarda TBMJ, Bobee B, Legendre P, Bruneau P. 1999. The Gumbel mixed model for flood frequency analysis. *Journal of Hydrology* **226**: 88–100.
Zuo D. 1991. *Selected works for environment change and water-sand dynamic law research* (Vol. 1). China Geology Press: Beijing; 45–97.

DOI: 10.1002/rra